Reprinted from JOURNAL OF THE ATMOSPHERIC SCIENCES, Vol. 38, No. 9, September 1981
American Meteorological Society
Printed in U. S. A.

A Method for Determining the Single Scattering Albedo of Clouds Through Observation of the Internal Scattered Radiation Field

MICHAEL D. KING

Laboratory for Atmospheric Sciences, Goddard Space Flight Center, NASA, Greenbelt, MD 20771

(Manuscript received 16 December 1980, in final form 13 May 1981)

ABSTRACT

A method is presented for determining the single scattering albedo of clouds at selected wavelengths in the visible and near-infrared wavelength regions. The procedure compares measurements of the ratio of the zenith to nadir propagating intensities deep within a cloud layer with radiative transfer computations of the same. Analytic formulas are derived which explicitly show the dependence of the internal intensity ratio on ground albedo, optical depth, single scattering albedo and cloud asymmetry factor. The single scattering albedo and cloud asymmetry factor enter the solution in such a way that a similarity relationship exists between these two parameters. As a result, the accuracy with which the single scattering albedo can be determined is dictated by the accuracy with which the asymmetry factor can be estimated. A method of observation is described whereby aircraft measurements of the zenith and nadir propagating intensities can be used to determine the similarity parameter as a function of wavelength. Since the fractional absorption of a cloud depends on the similarity parameter and not on the single scattering albedo and asymmetry factor separately, this poses no severe limitation to the method. An accurate knowledge of the ground albedo and total optical thickness of a cloud are unnecessary for a solution, provided one associates the wavelength for which the intensity ratio is a maximum with conservative scattering. Under this internal calibration approach, uncertainties in the ground albedo are very nearly compensated by uncertainties in the cloud optical thickness.

1. Introduction

The single scattering albedo of clouds is an important parameter affecting the transfer and deposition of radiant energy in the earth's atmosphere. In addition to water vapor, liquid (or ice) water particles and certain absorbing gases, aerosol particles within the cloud volume contribute to the absorption of solar radiation by clouds. Only a small fraction of all airborne particles participate directly in cloud formation by acting as nuclei for the condensation process. The airborne particles which do absorb energy, which are likely to be large insoluble and possibly hydrophobic particles, will initially be found in the air between the cloud drops. Twomey (1972) has shown that these absorbing particles will primarily remain interstitial to the cloud drops, even after a period of time during which some coagulation through diffusion and diffusiophoresis has occurred.

Twomey (1976) and Stephens (1978a,b) have examined the absorption of solar radiation in extended clouds composed of water vapor and liquid water and concluded that absorption approaches 15–20% for the more absorbing and thicker clouds, particularly when the sun is near the zenith. Stephens (1978a) further showed that of this absorption the contribution by liquid water is of the same order as water vapor, except for the optically thin clouds in the lower atmosphere. Davis *et al.* (1979a,b) examined the absorption of solar radiation by cubic clouds and found that at small (large) solar zenith angles finite clouds absorb less (more) radiation than in an equal volume element of horizontally infinite cloud. Considering the atmospheric column as a whole, Davis *et al.* (1979a) found that absorption is nearly equivalent for columns containing horizontally infinite clouds and columns containing finite clouds. They further noted that absorption is greater when a cloud is present than in the cloud-free case.

The few existing measurements of shortwave absorption by clouds have been obtained using broadband pyranometers flown above and below clouds. These measurements (Reynolds *et al.*, 1975; Stephens *et al.*, 1978) suggest a significant absorption of solar radiation by cloud layers, absorption often exceeding theoretical predictions for clouds composed solely of liquid water and water vapor. This led Twomey (1972, 1977) to suggest that absorbing aerosol particles may be partly responsible for this anomalous absorption, although the possibility also exists that leakage of radiation through the side walls of some of the real clouds could

also account for some of the large values of absorption implied by the measurements. Stephens *et al.* (1978) took care to present measurements for single-level clouds extensive enough to allow an aircraft to fly horizontally over or through them for several minutes, and sometimes up to several hours. They still found measured absorptions in excess of theoretical predictions, even for their three Hobart clouds which were their densest and most extensive clouds.

One of the difficulties in interring absorption properties by using radiometric observations external to a cloud is that these must be absolute measurements with a high degree of accuracy. In addition, horizontal inhomogeneities and the finite horizontal extent of many terrestrial clouds make it difficult to unambiguously separate the effects of true absorption from those of geometry, as pointed out by McKee and Cox (1974, 1976), Davies (1978) and Davis *et al.* (1979a,b), among others. Even for plane-parallel, horizontally homogeneous clouds of sufficient optical thickness ($\tau_c \geq 20$), the intensity distribution emerging from cloud base has the same asymptotic angular distribution whether the scattering process is conservative or slightly nonconservative, the only difference being in the magnitude of the intensity field (Sobolev, 1975). Only deep within a cloud layer does there appear to be an asymptotic angular distribution of scattered radiation which is both sensitive to absorption and simplified in character over that at either the top or bottom boundary of a cloud. This region, known as the diffusion domain, has recently been examined by Mel'nikova (1978) for the possibility of determining the single scattering albedo as a function of wavelength from hemispheric flux density measurements.

The intent of this paper is to demonstrate the sensitivity of the internal scattered radiation field to absorption by the cloud medium; and to demonstrate that this sensitive relationship provides a convenient tool for determining the single scattering albedo of a cloud. It will be demonstrated that the ratio of the zenith to nadir propagating intensities within a cloud layer can be measured as a function of wavelength and, with certain *a priori* information about the cloud asymmetry factor, compared to theoretical calculations to determine spectral values of the single scattering albedo of a cloud. A method of observation and analysis will be described from which necessary data can be obtained by an aircraft-based instrumentation system.

2. Radiation field in deep layers

From a position deep within an optically thick, plane-parallel and horizontally infinite cloud, the radiation is transported by the simplest diffusion mode as if the cloud were unbounded. In this region, known as the diffusion domain, the role of direct (unscattered) radiation is negligible compared to the role of diffuse radiation and the intensity of radiation does not depend on azimuth angle. For the case of a vertically homogeneous cloud characterized by a single scattering albedo $\omega_0 < 1$, it is well known (see, e.g., van de Hulst, 1968a, 1980) that the intensity in the diffusion domain is given by

$$I_{\text{atm}}(\tau,u) = s_1 P(u) e^{-k\tau} + s_2 P(-u) e^{k\tau}. \qquad (1)$$

In this expression τ is the normal optical depth measured into the cloud from the top boundary, u the direction cosine with respect to the positive τ direction ($-1 \leq u \leq 1$), $P(u)$ the diffusion pattern, k the diffusion exponent, and s_1 and s_2 the strengths of the diffusion streams in the positive and negative τ directions, respectively.

The main features to be observed in (1) are that, given sufficient optical depth, the energy transport process will settle down to a fixed angular pattern and fixed damping, independent of solar zenith angle, and that this damping is not as strong as in a straight beam (i.e., $0 \leq k \leq 1$). The depth at which (1) applies in a cloud of total optical thickness τ_c will be discussed in Section 5, where it will be shown that this depth is dependent on the cloud asymmetry factor g.

The diffusion pattern and diffusion exponent, as well as other functions and constants arising in asymptotic expressions for the emerging and internal intensities of very thick layers, can easily be determined by applying the asymptotic fitting method of van de Hulst (1968b). In this method, computational results from the doubling method are fit to known general forms of the asymptotic equations [such as Eq. (1) for $\tau = \tau_c/2$]. The form of the doubling method used in the present investigation was that described by Hansen (1971) and Hansen and Travis (1974), where it was necessary to consider only azimuth-independent radiation. Since van de Hulst (1980) shows that the value of the diffusion exponent and form of the diffusion pattern are virtually unaltered if polarization is neglected, we have further chosen to neglect polarization. The starting point was an initial layer sufficiently thin that single scattering could be assumed (in this case $\tau_0 = 2^{-30}$). Alternative initializations have been used and discussed by Wiscombe (1976, 1977) and Kattawar and Plass (1973) but have not been incorporated in the present investigation.

All the results presented in this paper were obtained using the phase function first introduced by Henyey and Greenstein (1941) and given by

$$\Phi(\cos\Theta) = \frac{1 - g^2}{(1 + g^2 - 2g\cos\Theta)^{3/2}}, \qquad (2)$$

where g is the asymmetry factor and Θ the scattering angle. This is a convenient phase function to use in radiative transfer modeling studies of clouds since it allows the variation of g and ω_0 separately, and since the scattering and absorption properties of optically thick clouds are determined primarily by τ_c, ω_0 and g (see, e.g., van de Hulst, 1980). Since the range of values of g in terrestrial clouds is roughly $0.80 \leq g \leq 0.90$ in the visible and near-infrared regions (Twomey, 1974), computations have further been restricted to this domain. For water clouds in the visible wavelength region where the refractive index $m = 1.33-0.00i$, the upper limit of g from Mie theory is 0.884 (Irvine, 1963) with larger values being possible only for large particles in the near-infrared due to finite absorption by the particles.

The diffusion pattern, which obeys the normalization condition

$$\frac{1}{2}\int_{-1}^{1} P(u)du = 1, \tag{3}$$

is illustrated in Fig. 1 as a function of u for various values of ω_0 when $g = 0.85$. In this figure it was convenient to plot $P(u)$ relative to $P(1)$, representing downwelling photons from the zenith. It is evident from Fig. 1 that $P(u)$ is a strong function of ω_0 with the largest value for nadir propagating photons ($u = 1$) and the smallest value for zenith propagating photons ($u = -1$). For conservative scattering $P(u) = 1$, being everywhere isotropic. The range of single scattering albedos illustrated in Fig. 1 (i.e., $0.9 \leq \omega_0 \leq 1.0$) covers the range of values expected in terrestrial clouds in the visible and near-infrared regions, at least in the absence of appreciable absorption by aerosol particles (see, e.g., Twomey, 1976; Twomey and Seton, 1980). Over this range $P(u)$ is a monotonically increasing function of u, even for phase functions other than Henyey-Greenstein (see Kattawar and Plass, 1976).

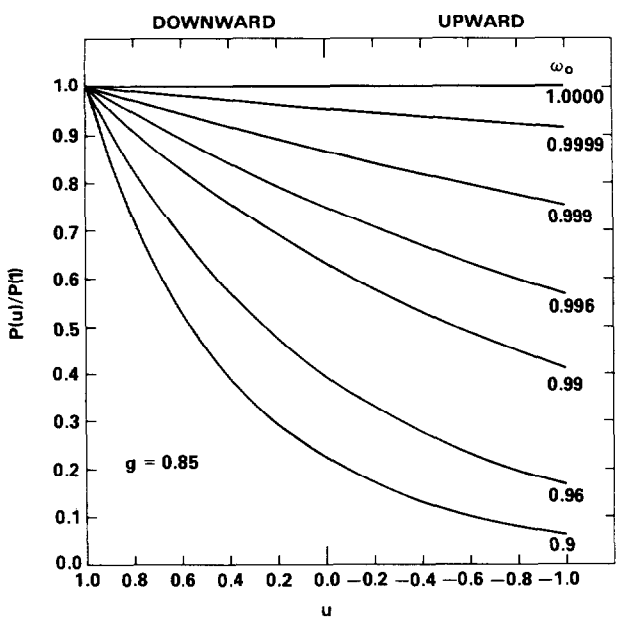

FIG. 1. Diffusion pattern as a function of the cosine of the zenith angle u for a Henyey-Greenstein phase function with $g = 0.85$ and for seven values of the single scattering albedo. All curves are normalized to unity for downwelling photons from the zenith.

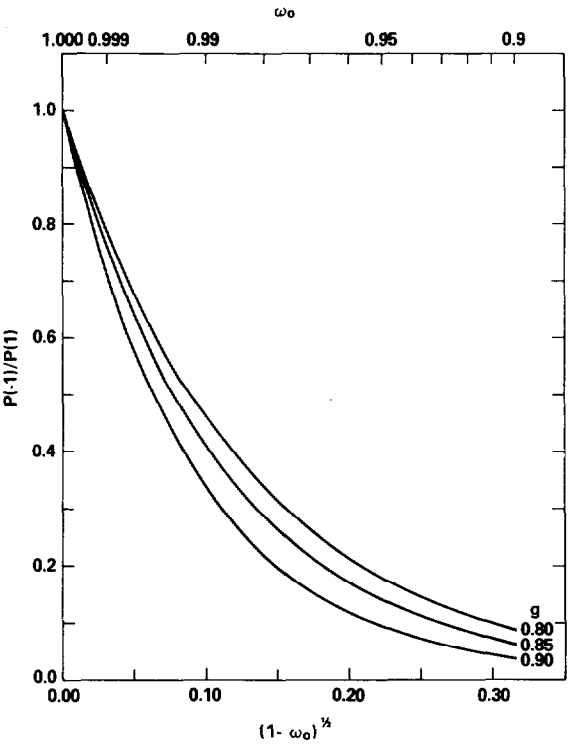

FIG. 2. Diffusion pattern ratio as a function of $(1 - \omega_0)^{1/2}$ for three values of the asymmetry factor.

Fig. 2 illustrates $P(-1)/P(1)$ as a function of $(1 - \omega_0)^{1/2}$ for three different values of the asymmetry factor, *viz.*, 0.80, 0.85 and 0.90. This ratio,

$$D = P(-1)/P(1), \tag{4}$$

termed the diffusion pattern ratio, shows the required sensitivity to ω_0 as well as a sensitivity to g. It represents the ratio of the zenith to nadir propagating intensities deep within a semi-infinite atmosphere. It will be shown in Section 4 that the appropriate choice of a function of both ω_0 and g can make all the curves in Fig. 2 essentially coincide. From the well-known power series expansion of $P(u)$ given by van de Hulst (1968a), it is easy to show that for small absorption D varies linearly with $(1 - \omega_0)^{1/2}$ with a slope of $-[12/(1 - g)]^{1/2}$ and an intercept of 1.0, in agreement with Fig. 2 for $(1 - \omega_0)^{1/2} \leq 0.03$.

With the $\tau = 0$ level taken as the top boundary

of the cloud, van de Hulst (1968a) shows that

$$s_2 = -ls_1 e^{2k\tau_c}, \tag{5}$$

where l is a positive constant known as the negative internal reflection coefficient, defined as a two-way transmission to a virtual optical depth q beneath the base of the cloud. Thus

$$l = e^{-2kq}, \tag{6}$$

where q is the extrapolation length. Combining (5) with (1), and recalling the definition in (4), it immediately follows that the ratio of the zenith propagating to nadir propagating intensity in the diffusion domain is given by

$$\frac{I_{\text{atm}}(\tau, -1)}{I_{\text{atm}}(\tau, 1)} = \frac{D - le^{-2k(\tau_c - \tau)}}{1 - Dle^{-2k(\tau_c - \tau)}}. \tag{7}$$

This expression naturally reduced to D for a semi-infinite atmosphere, as required.

When $\omega_0 = 1$ Eq. (7) is indeterminate since $D = l = 1$ and $k = 0$. The solution for this special case follows readily from the expression for the internal intensity field in the diffusion domain for conservative scattering, which can be obtained from the power series expansion of $P(u)$ given by van de Hulst (1968a, 1980). Substituting this expression into (1) leads to

$$I_{\text{atm}}(\tau, u) = \frac{\mu_0 F_0 K(\mu_0)}{\pi(1 - g)(\tau_c + 2q_0)} \times [(1 - g)(\tau_c - \tau + q_0) + u], \tag{8}$$

from which it immediately follows that

$$\frac{I_{\text{atm}}(\tau, -1)}{I_{\text{atm}}(\tau, 1)} = \frac{(1 - g)(\tau_c - \tau + q_0) - 1}{(1 - g)(\tau_c - \tau + q_0) + 1}. \tag{9}$$

In these expressions F_0 is the solar flux density incident on the top of the atmosphere, $K(\mu_0)$ the escape function, and q_0 the extrapolation length for conservation scattering, where $q' = (1 - g)q_0$ is known to range between 0.709 and 0.715 for all possible phase functions (van de Hulst, 1980). Herman *et al.* (1980) recently presented numerical results for the azimuthally independent intensity within optically thick, conservatively scattering, media. Their results clearly demonstrate the transition to a diffusion domain well described by (8), where the intensity depends linearly on both τ and u. Although (8) represents the unpolarized solution for the internal intensity in the diffusion domain for conservative scattering, it should be noted that it *also* holds for conservative scattering with polarization (van de Hulst, 1980).

By measuring both the nadir intensity and zenith intensity with the same instrument, as suggested here, it is not necessary to have an absolute calibration of the instrument. It is also unnecessary to know the extraterrestrial solar flux density or solar zenith angle precisely, since these parameters affect only the magnitude of the intensity (through s_1 and s_2) and not the relative angular distribution [cf. Eqs. (7) and (9)]. The escape (or injection) function $K(\mu_0)$, which also enters the expression for s_1 and s_2, is a function not only of the cosine of the solar zenith angle μ_0, but also of ω_0, which is not known *a priori*. Analogous expressions to (7) and (9) for the ratios of hemispheric flux densities can easily be derived (see, e.g., Mel'nikova, 1978) but flux densities are much more difficult to measure accurately in narrow spectral intervals than are intensities. An instrument such as the one described by King (1979) might be necessary for measuring flux densities, and even then it is difficult to look up and down with the same instrument from an aircraft platform. Intensities, in principle, could be measured with a simple scanning radiometer followed by a spectrometer, so that both zenith and nadir intensities are measured with the same optical system and detectors.

From any arbitrary level τ of sufficient distance from both the top and bottom boundaries of a cloud such that the necessary characteristics of the diffusion domain are established, the ratio $I_{\text{atm}}(\tau, -1)/I_{\text{atm}}(\tau, 1)$ is a monotonically decreasing function as $(1 - \omega_0)^{1/2}$ increases. This can be seen on examination of Fig. 3 for the cases in which the ground albedo $A_g = 0.0$. These curves apply at the mid-level of clouds of total optical thickness 32, 64 and 128, where the clouds are again assumed to scatter radiation with the Henyey-Greenstein phase function with $g = 0.85$. It is clear from Fig. 3 that the wavelength for which this ratio is the largest corresponds to the wavelength for which ω_0 is the closest to unity. If one assumes that $\omega_0 = 1$ at this wavelength, then (9) can immediately be used to solve for $(1 - g)(\tau_c - \tau)$. Since the sensitivity of the intensity ratio to absorption decreases dramatically for nearly conservative scattering, as apparent on examination of Fig. 3, little uncertainty arises in the estimation of $(1 - g)(\tau_c - \tau)$ even if no wavelength has precisely conservative scattering. Use of this internal calibration approach negates the need to know the τ level of the aircraft or indeed the total optical thickness of the cloud, and assures that $\omega_0 = 1$ at some wavelength, or number of wavelengths, in the visible wavelength region. The function $(1 - g)(\tau_c - \tau)$ can further be used to estimate whether the diffusion domain has been established, as discussed in Section 5. Substitution of $(1 - g)(\tau_c - \tau)$ into (7) shows that the ratio $I_{\text{atm}}(\tau, -1)/I_{\text{atm}}(\tau, 1)$ at all other wavelengths is a function of D, l and $k/(1 - g)$, each of which is strongly ω_0 dependent (see Section 4).

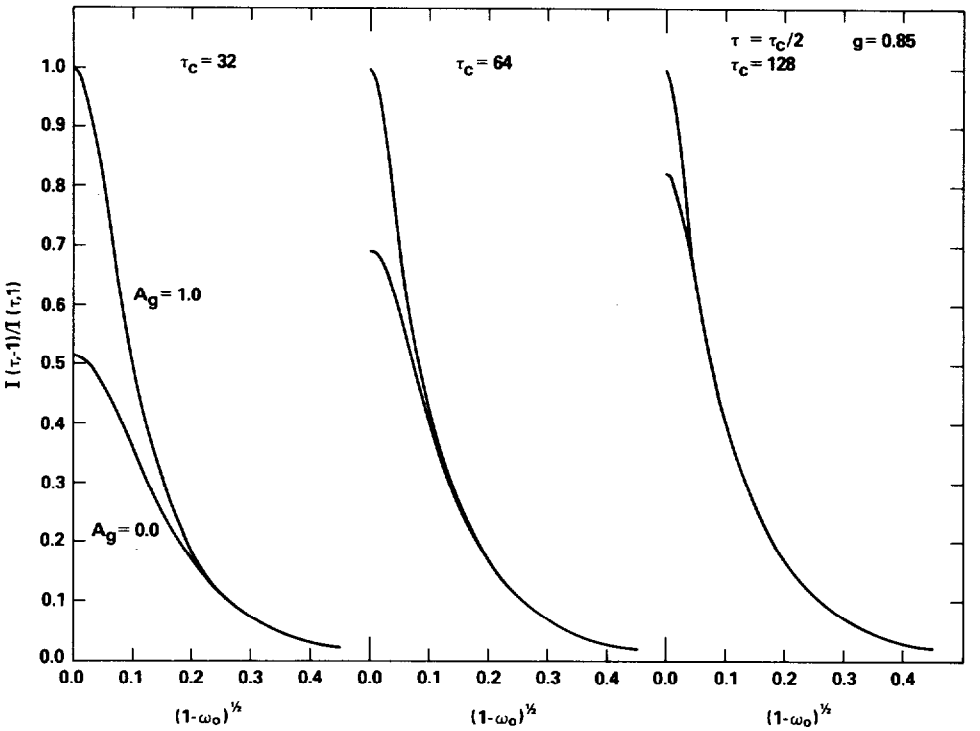

FIG. 3. Ratio of the zenith to nadir propagating intensities at the mid-level of a cloud as a function of $(1 - \omega_0)^{1/2}$, τ_c and A_g. These curves apply for a Henyey-Greenstein phase function with g = 0.85.

3. Influence of surface reflection

In the previous section, reflection of the transmitted radiation by the underlying surface was neglected. The extension of Eqs. (7) and (9) to include not only plane-parallel illumination from above the cloud but also diffuse radiation from below, can easily be accomplished for cases when the surface is assumed to reflect radiation according to Lambert's law with some albedo A_g. Chandrasekhar was the first to derive expressions for the effect of a Lambertian surface on the reflected and transmitted intensities in a planetary atmosphere (see Chandrasekhar, 1950). In addition to the intensities emerging from the upper and lower boundaries of an atmosphere, it is possible to derive expressions for the effect of ground reflection on the intensity field at any arbitrary level τ within an atmosphere.

Adopting the notation of van de Hulst (1980), one can readily show that the azimuthally independent intensities in the upward and downward directions are given, respectively, by

$$I^0(\tau, -\mu, \mu_0) = I^0_{\text{atm}}(\tau, -\mu, \mu_0) + \frac{A_g}{1 - A_g A^*(\tau_c)} \mu_0 t_{\text{atm}}(\tau_c, \mu_0) \times \left[2 \int_0^1 I^0_{\text{atm}}(\tau_c - \tau, \mu, \mu') d\mu' + F_0 \pi^{-1} e^{-(\tau_c - \tau)/\mu} \right], \quad (10)$$

$$I^0(\tau, \mu, \mu_0) = I^0_{\text{atm}}(\tau, \mu, \mu_0) + \frac{A_g}{1 - A_g A^*(\tau_c)} \mu_0 t_{\text{atm}}(\tau_c, \mu_0) \times 2 \int_0^1 I^0_{\text{atm}}(\tau_c - \tau, -\mu, \mu') d\mu'. \quad (11)$$

In these expressions $I^0_{\text{atm}}(\tau, -\mu, \mu_0)$ and $I^0_{\text{atm}}(\tau, \mu, \mu_0)$ are the upward and downward intensities in the absence of ground reflection; μ the direction cosine with respect to the local normal, either in or out ($\mu = |u|$); and $A^*(\tau_c)$ and $\mu_0 F_0 t_{\text{atm}}(\tau_c, \mu_0)$ the spherical albedo and transmitted flux density (diffuse plus direct) when $A_g = 0$. $A^*(\tau_c)$ and $t_{\text{atm}}(\tau_c, \mu_0)$ are equivalent to $\bar{s}(\tau_c)$ and $\gamma_1(\tau_c, \mu_0)$ in Chandrasekhar's (1950) notation, respectively.

Eqs. (10) and (11) contain no assumptions about the thickness of the atmosphere, applying equally well to thin or thick atmospheres at any level τ within or at the boundaries of an atmosphere. In addition to reducing to the well-known expressions for the reflected [Eq. (10), $\tau = 0$] and transmitted [Eq. (11), $\tau = \tau_c$] intensities, Eqs. (10) and (11) admit

the necessary boundary conditions

$$I^0(0, \mu, \mu_0) = 0,$$

$$\pi I^0(\tau_c, -\mu, \mu_0) = \frac{A_g}{1 - A_g A^*(\tau_c)} \mu_0 F_0 t_{\text{atm}}(\tau_c, \mu_0).$$

In the doubling method of solving the radiative transfer equation, the reflection and transmission functions of a single layer of optical thickness $\tau_c/2$ are combined with those of a similar layer to obtain the reflection and transmission functions of the combined layer of optical thickness τ_c. In performing this doubling a necessary computational step is the computation of the internal intensity field at the boundary of the two layers (i.e., the $\tau = \tau_c/2$ level of an atmosphere of total optical thickness τ_c). Combining this result with (10) and (11) permits the computation of $I^0(\tau_c/2, u, \mu_0)$ for any desired optical thickness and ground albedo. This affords a convenient check on the accuracy of the results developed below.

As τ_c becomes large and one is positioned within the diffusion domain, far from both the top and bottom boundaries of a cloud, the directly transmitted term in (10) becomes negligible compared to the diffuse term. Combining (10) and (11) with the expressions for the intensity field in the diffusion domain in the absence of ground reflection, given by (1) for $\omega_0 < 1$ and (8) for $\omega_0 = 1$, it can be shown that

$$I(\tau, u, \mu_0) = I_{\text{atm}}(\tau, u, \mu_0) + \frac{A_g}{1 - A_g A^*(\tau_c)} \times \frac{n t_{\text{atm}}(\tau_c, \mu_0)}{K(\mu_0)} I_{\text{atm}}(\tau_c - \tau, -u, \mu_0), \quad (12)$$

where the superscript has been deleted since the intensity field in the diffusion domain is azimuthally independent and no further azimuthal terms exist. In deriving this expression, use was made of (5) as well as the explicit expression for s_1, given by (van de Hulst, 1968a)

$$s_1 = \frac{\mu_0 F_0 K(\mu_0)}{\pi(1 - f^2)}, \quad (13)$$

where

$$f = l e^{-k\tau_c}. \quad (14)$$

The constant n represents the μ weighted mean value of the escape function $K(\mu)$ and is defined by

$$n = 2 \int_0^1 K(\mu) \mu d\mu. \quad (15)$$

Eq. (12) applies equally well to conservative scattering as to nonconservative scattering, where in the former case $n = 1$. Before proceeding to expressions for the ratio of the zenith propagating to nadir propagating intensities in the diffusion domain, further simplifications can be obtained by making use of asymptotic expressions for $A^*(\tau_c)$ and $t_{\text{atm}}(\tau_c, \mu_0)$, given by

$$t_{\text{atm}}(\tau_c, \mu_0) = \frac{4K(\mu_0)}{3(1 - g)(\tau_c + 2q_0)}, \quad (16)$$

$$A^*(\tau_c) = 1 - \frac{4}{3(1 - g)(\tau_c + 2q_0)}, \quad (17)$$

for $\omega_0 = 1$ and

$$t_{\text{atm}}(\tau_c, \mu_0) = \frac{mn}{1 - f^2} K(\mu_0) e^{-k\tau_c}, \quad (18)$$

$$A^*(\tau_c) = A^* - \frac{mn^2}{1 - f^2} l e^{-2k\tau_c}, \quad (19)$$

for $\omega_0 < 1$. In these expressions A^* is the spherical (Bond) albedo of a semi-infinite atmosphere; m a constant given by

$$m = 2 \int_{-1}^1 [P(u)]^2 u du; \quad (20)$$

and all other functions and constants have previously been defined.

One observes from (16) and (18) that the ratio $t_{\text{atm}}(\tau_c, \mu_0)/K(\mu_0)$ which enters (12) is not a function of μ_0. This implies that the relative angular distribution of the intensity in the diffusion domain is independent of μ_0, as in the previous section, but that the absolute magnitude of the intensity is still proportional to $\mu_0 K(\mu_0)$ through s_1. Combining (12), (16) and (17) with (8), it can be shown after some algebraic manipulation that the ratio of the zenith to nadir propagating intensities in the diffusion domain for conservative scattering ($\omega_0 = 1$) is given by

$$\frac{I(\tau, -1)}{I(\tau, 1)} = \frac{3(1 - A_g)[(1 - g)(\tau_c - \tau + q_0) - 1] + 4A_g}{3(1 - A_g)[(1 - g)(\tau_c - \tau + q_0) + 1] + 4A_g} \quad (21)$$

where the explicit dependence of the intensities on μ_0 has been deleted. When $A_g = 0$ this expression necessarily reduces to (9) and when $A_g = 1$ the intensity ratio becomes unity, as in a semi-infinite atmosphere.

For nonconservative scattering the ratio of the zenith to nadir propagating intensities in the diffusion domain can be obtained from (12), (18), (19) and (1), where (5) is used to determine the relative strengths of the two diffusion streams. The result can be obtained in the form

$$\frac{I(\tau, -1)}{I(\tau, 1)} = \frac{(1 - A_g A^*)[D - le^{-2k(\tau_c - \tau)}] + A_g mn^2 e^{-2k(\tau_c - \tau)}}{(1 - A_g A^*)[1 - Dle^{-2k(\tau_c - \tau)}] + A_g mn^2 De^{-2k(\tau_c - \tau)}}. \quad (22)$$

When $A_g = 0$ this expression reduces to (7) and for a semi-infinite atmosphere to D, as required.

Fig. 3 illustrates $I(\tau, -1)/I(\tau, 1)$ as a function of $(1 - \omega_0)^{1/2}$ at the mid-level of clouds of total optical thickness 32, 64 and 128. Only curves for the two ground albedos $A_g = 0.0$ and 1.0 are illustrated, other results lying between these two extremes. The results presented in Fig. 3 were obtained from the doubling method at the boundary of the two combined layers by making use of the exact expressions (10) and (11). At $\tau_c = 32$ the ratio of the zenith to nadir propagating intensities is slightly μ_0 dependent (see Section 5), becoming insensitive to μ_0 to at least five significant figures when $\tau_c = 64$ and 128. The results illustrated in Fig. 3 for $\tau_c = 32$ correspond to a solar zenith angle of 35° ($\mu_0 = 0.819$), which is the solar zenith angle for which $I(\tau, -1)/I(\tau, 1)$ generally agrees the closest with (21) and (22). Comparison of the solutions represented by these equations with those illustrated in Fig. 3 shows overall agreement to within the width of the lines in the figure, where all functions and constants appearing in (21) and (22) were obtained by the asymptotic fitting method of van de Hulst (1968b, 1980).

In addition to being monotonically decreasing as absorption increases, the ratio of the zenith to nadir propagating intensities in the diffusion domain is a smooth function generally having the steepest slope for small values of $1 - \omega_0$. This means that the intensity ratio in the diffusion domain is unusual in that it is the most sensitive to absorption for single scattering albedos in the range $0.9 \leq \omega_0 \leq 0.9999$, those most often believed to exist in terrestrial clouds in the near-infrared. Flux divergence between two different heights in the atmosphere, as occasionally measured by aircraft, is subject to large errors for small absorption since analysis requires taking the difference of two large flux measurements in order to obtain a small residual flux lost to absorption. When the single scattering albedo is less than 0.8, not only is the intensity ratio small and relatively insensitive to ω_0 but also the magnitude of the intensity becomes too small to be practical for measurement (Kattawar and Plass, 1975). In terrestrial clouds composed of water or ice particles, it is unlikely that ω_0 will be as small as 0.8 except in the bands of strong molecular absorption. In the ocean, on the other hand, values of $\omega_0 \leq 0.8$ are likely at many wavelengths.

The sensitivity of the intensity ratio to total optical thickness and ground albedo is also illustrated in Fig. 3, where it is apparent that the effect of surface reflection decreases as either the total optical thickness or cloud absorption increases. This is due to less radiation being transmitted through the cloud to be reflected by the surface.

4. Similarity relations

In addition to being a monotonically decreasing function as $(1 - \omega_0)^{1/2}$ increases, the intensity ratio increases with height above the base of the cloud, provided only that the level τ is of sufficient distance from the top and bottom boundaries of the cloud for the diffusion domain to be established. This is evident from (21) and (22), where the ratio of the zenith to nadir propagating intensities is shown to be a function of the *difference* in optical depth between the base of the cloud and any arbitrary level within the cloud. This suggests that an entirely equivalent interpretation of Fig. 3 is that all curves refer to a single cloud of total optical thickness $\tau_c = 128$ and that the three families of curves refer in turn to levels $\tau_c - \tau = 16$, 32 and 64. This implies that high in a cloud there is less sensitivity of the intensity ratio to surface reflection than low in a cloud, and that the sensitivity of the intensity ratio to ω_0 increases with height.

In addition to A_g and $(1 - g)(\tau_c - \tau)$, the intensity ratio for conservative scattering [Eq. (21)] is a function of $(1 - g)q_0$, which is known to range between 0.709 and 0.715 for all possible phase functions (van de Hulst, 1980). Since clouds are expected to have phase functions characterized by asymmetry factors within a restricted range, this range of $(1 - g)q_0$ can further be narrowed such that it is sufficiently accurate to let

$$(1 - g)q_0 = 0.714. \quad (23)$$

This value was obtained by applying the asymptotic fitting method to doubling computations using the Henyey-Greenstein phase function, from which we find that the values of $(1 - g)q_0$ fall in the narrow range 0.7137–0.7143 for $0.80 \leq g \leq 0.90$.

For wavelengths ≥ 0.75 μm the single scattering albedo of clouds is less than unity. At these wavelengths the intensity ratio is seen from (22) to be a function of A^*, D, l, $k/(1 - g)$, m and n, in addition to being a function of A_g and $(1 - g)(\tau_c - \tau)$. Each of these six constants (A^*, D, . . . , n) is strongly ω_0 dependent with a somewhat weaker dependence on g (at least for $0.80 \leq g \leq 0.90$). Strictly speaking, we would expect each constant to depend on all expansion coefficients of the phase function, not only on ω_0 and g, but since each constant is based on the properties of a semi-infinite atmosphere it turns out that the higher expansion coefficients are quite insignificant, particularly when $1 - \omega_0 \ll 1$.

van de Hulst (1974) examined this question of similarity for the spherical albedo A^* of a semi-infinite atmosphere and found that A^* can be well

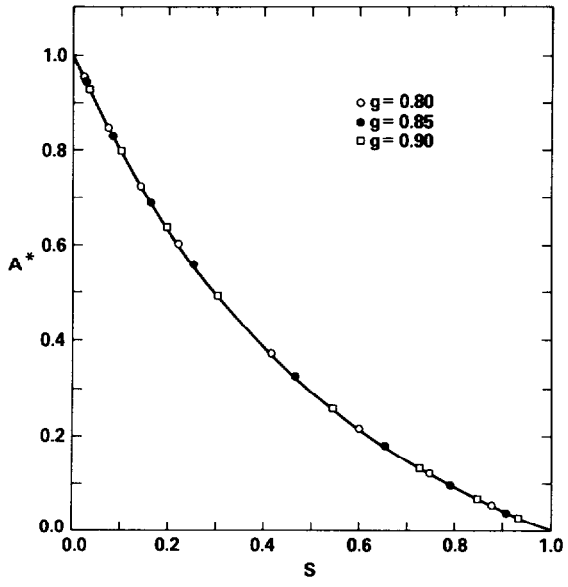

FIG. 4. Spherical albedo A^* of a semi-infinite atmosphere as a function of similarity parameter $s = [(1 - \omega_0)/(1 - \omega_0 g)]^{1/2}$. The symbols represent values obtained by numerical computation and the curve the result of a least-squares fit to an analytic equation.

described by a function of a similarity parameter s, defined by

$$s = \left(\frac{1 - \omega_0}{1 - \omega_0 g}\right)^{1/2}. \tag{24}$$

This parameter has the property of reducing to $(1 - \omega_0)^{1/2}$ for isotropic scattering and of spanning the range 0 ($\omega_0 = 1$) to 1 ($\omega_0 = 0$). Each of the constants A^*, D, l, $k/(1 - g)$, m and n can be expanded in power series in s, such as

$$A^* = 1 - (4/\sqrt{3})s + 4(1 - g)q_0 s^2 + O(s^3), \tag{25}$$

$$D = 1 - 2\sqrt{3}s + 6s^2 + O(s^3), \tag{26}$$

$$m = (8/\sqrt{3})s + O(s^3), \tag{27}$$

where $O(s^3)$ denotes terms of order s^3 or higher. These expressions become increasingly more accurate for small values of s (i.e., $\omega_0 \geq 0.995$).

Since it is desirable to have expressions for these constants over a much wider range of s (and hence ω_0), computations of each of these constants were performed for the set of Henyey-Greenstein phase functions with $\omega_0 = 0.9999, 0.999, 0.996, 0.99, 0.96, 0.9, 0.8, 0.6$ and $g = 0.80, 0.85, 0.90$. These results were obtained by the asymptotic fitting method and are presented in Figs. 4–9. It is clear that each of these constants is primarily a function of s over the entire range $0 \leq s \leq 1$. van de Hulst (1974) noted this similarity in A^* and later (van de Hulst, 1980) in l, but it is clear that the other four constants and functions appearing in the expression for the intensity ratio in deep layers {*viz.*, D, $\exp[-k/(1 - g)]$, n^2 and m} also obey similarity relations, at least for $0.80 \leq g \leq 0.90$. It is clear on examination of Figs. 2 and 5 that the choice of similarity parameter defined by (24) makes all curves in Fig. 2 virtually coincide. The similarity relation for $k/(1 - g)$ could be substantially improved at large values of s over a wide range of g values by selecting $k/(1 - \omega_0 g)$, rather than $k/(1 - g)$. This would lead to a sensitivity of the intensity ratio to s and $(1 - \omega_0 g)(\tau_c - \tau)$, the latter variable being dependent on ω_0 and hence more wavelength de-

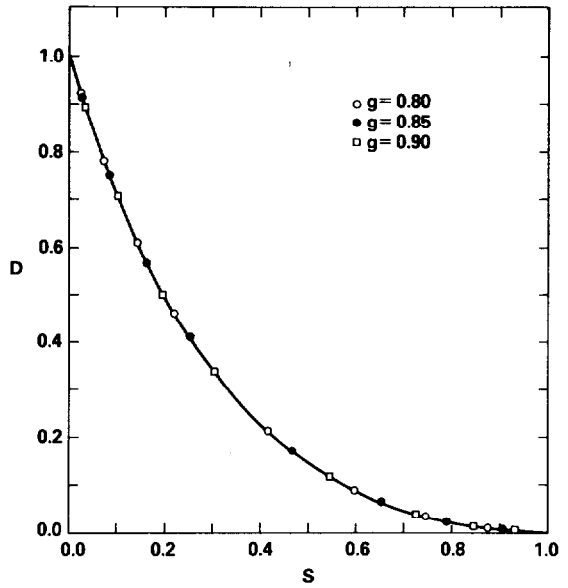

FIG. 5. As in Fig. 4 except for the diffusion pattern ratio $D = P(-1)/P(1)$. These results are to be compared with Fig. 2.

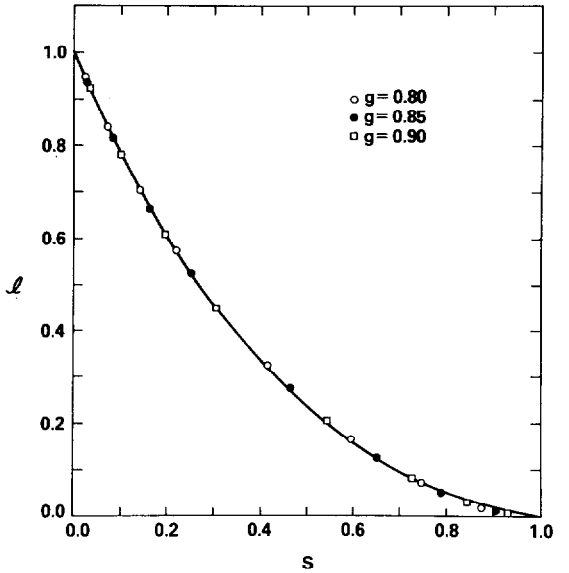

FIG. 6. As in Fig. 4 except for the negative internal reflection coefficient l.

pendent than $(1 - g)(\tau_c - \tau)$. Since cloud asymmetry factors lie in a relatively narrow range and since $k/(1 - g)$ enters (22) as an exponential $\exp[-k/(1 - g)]$, it is sufficiently accurate to scale k by the simpler relationship $k/(1 - g)$.

Since power series expansions of the six constants illustrated in Figs. 4–9, such as those given by (25)–(27), require an increasingly large number of terms as $s \geq 0.1$, it is advantageous to find empirical equations to fit each constant as a function of s over the full range $0 \leq s \leq 1$. A^*, D, l, $\exp[-k/(1 - g)]$ and n^2 were each fit to an equation of the form

$$\hat{y}(s) = \left[\frac{(1 + a_1 s)(1 - s)}{(1 + a_2 s)}\right]^{(1+a_3 s)}, \qquad (28)$$

where the choice of the factor $1 - s$ assures that the function vanishes at $\omega_0 = 0$, $s = 1$. This function, which also has the property that it equals unity at $\omega_0 = 1$, $s = 0$, was introduced by van de Hulst (1974) for the specific case where $a_3 = 0$. By combining (28) with (25) van de Hulst (1974) derived values for a_1 and a_2. As an alternative, we have chosen to use the computations presented in Figs. 4–8, together with the gradient-expansion method from nonlinear least-squares theory (Bevington, 1969, pp. 232–242), to determine the coefficients a_1, a_2 and a_3. These results are presented in Table 1 together with values of the statistic χ^2, defined as

$$\chi^2 = \sum_{i=1}^{N} [y_i - \hat{y}(s_i)]^2. \qquad (29)$$

In this expression y_i represents the computations of A^*, D, l, $\exp[-k/(1 - g)]$ and n^2 at each of the $N = 24$ values of s_i, respectively.

In order to find an empirical formula which gives a satisfactory fit to m as a function of s, consider-

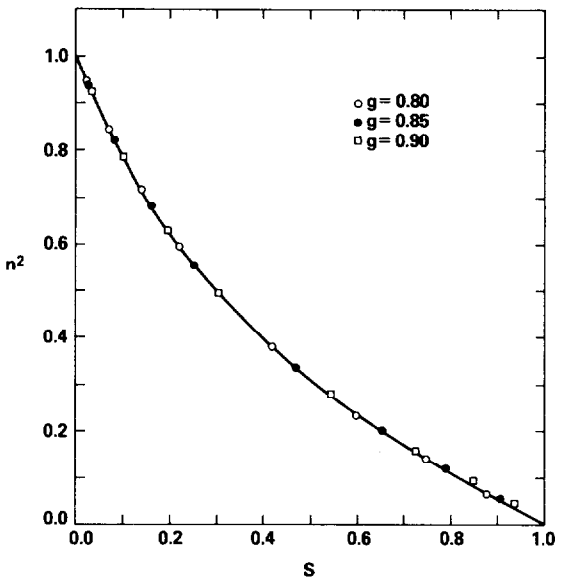

FIG. 8. As in Fig. 4 except for the constant n^2, where n is defined by Eq. (15).

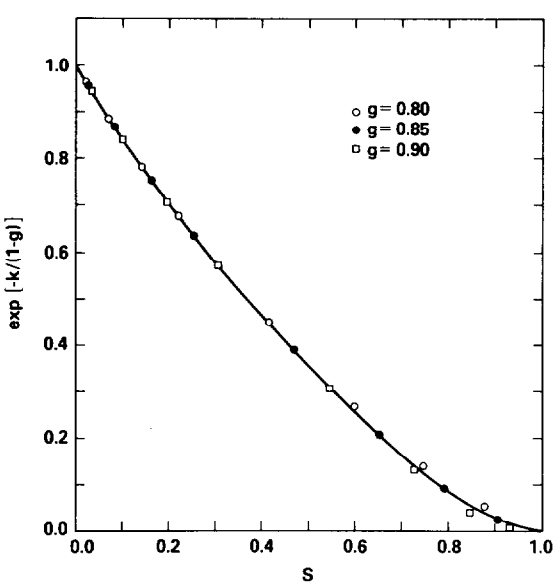

FIG. 7. As in Fig. 4 except for $\exp[-k/(1 - g)]$, where k is the diffusion exponent.

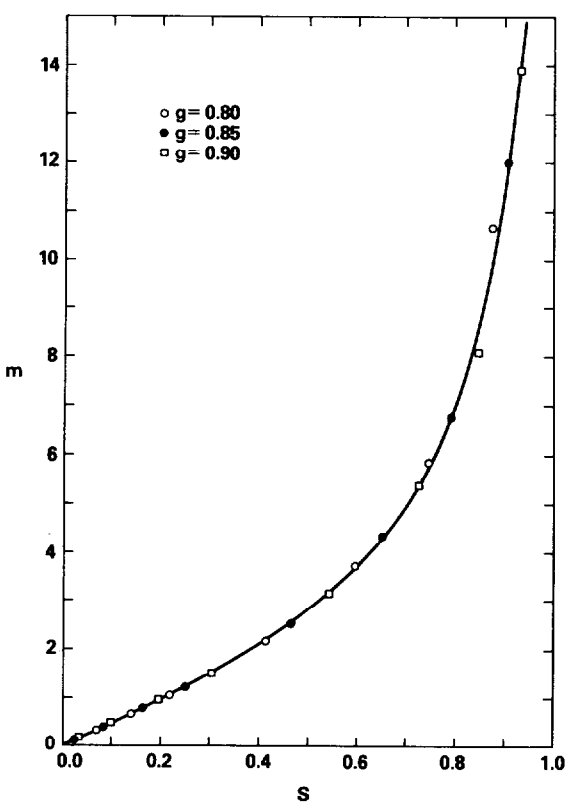

FIG. 9. As in Fig. 4 except for the constant m, defined by Eq. (20).

TABLE 1. Values of the coefficients a_1, a_2 and a_3 which give the best fit of the specified functions to an equation of the form of (28). The values of chi-square χ^2 for each fit are also given.

Function	a_1	a_2	a_3	χ^2
A^*	−0.161	1.139	0.000	4.921×10^{-6}
D	−0.979	1.503	0.000	8.258×10^{-6}
l	−0.788	0.566	0.000	5.033×10^{-4}
$\exp[-k/(1-g)]$	3.459	4.329	0.480	1.288×10^{-3}
n^2	0.598	2.169	0.000	3.587×10^{-4}

able experimentation was required. By fitting (28) to $\exp(-m)$ an accurate fit can be obtained for small values of s but this fit becomes unsatisfactory for $s \geqslant 0.5$. Alternatively m can be fit directly to the negative logarithm of (28), but this fit becomes unsatisfactory for $s \leqslant 0.5$. Based on the results of these two fits and the constraint that the fitting equation must reduce to (27) for small values of s, the following equation has been adopted:

$$\hat{m}(s) = (1 + 1.537s) \times \ln\left[\frac{1 + 1.800s - 7.087s^2 + 4.740s^3}{(1 - 0.819s)(1 - s)^2}\right]. \quad (30)$$

The fit represented by this equation as well as the fits obtained from (28) using the coefficients in Table 1 are presented as smooth curves in Figs. 4–9.

5. Determination of single scattering albedo

For wavelengths at which absorption due to water vapor, oxygen and liquid (or ice) water particles can be neglected, the only likely contributors to the absorption of solar radiation by clouds are aerosol particles within the cloud volume. Assuming that the ground albedo A_g is not strongly wavelength dependent over a relatively narrow region in the visible (e.g., $0.50 \leqslant \lambda \leqslant 0.75$ μm), the wavelength for which the ratio of the zenith to nadir propagating intensities deep within a cloud layer is the largest corresponds to the wavelength for which ω_0 is the closest to unity. If one assumes that $\omega_0 = 1$ at this wavelength, then spectral measurements of the intensity ratio in the diffusion domain contain enough information to obtain $(1-g)(\tau_c - \tau)$ and spectral values of s, the only thing being required is an estimate of A_g as a function of wavelength.

Fig. 10 illustrates $I(\tau,-1)/I(\tau,1)$ as a function of $(1-g)(\tau_c - \tau)$ for $A_g = 0.2$ and for four values of s. This figure represents the generalization of Fig. 3 to include arbitrary values of g, τ and τ_c, provided only that the observations are made at sufficient distance from the top and bottom boundaries of the cloud for the characteristics of the diffusion domain to be established. The computations presented in Fig. 10 were obtained using the doubling solution at the level $\tau = \tau_c/2$, together with (10) and (11) to account for surface reflection. The separation of each of the curves at values of $(1-g)(\tau_c - \tau) \leqslant 2.5$ reflects primarily the effects of solar zenith angle on the intensity ratio when τ_c is small, where the smallest intensity ratio occurs for overhead sun ($\mu_0 = 1$) and the largest intensity ratio for $\mu_0 \sim 0.5$. Obviously when $(1-g)(\tau_c - \tau) \leqslant 2.5$ but $(1-g)\tau \gg 2.5$ there would be no effect of the solar zenith angle on the intensity ratio, but the intensity field would be altered from that expected within the diffusion domain due to the proximity to the bottom boundary of the cloud. Thus it is safest to restrict measurements of the zenith and nadir intensities to the levels

$$\frac{2}{(1-g)} \leqslant \tau \leqslant \tau_c - \frac{2}{(1-g)}. \quad (31)$$

By employing various methods of solving the radiative transfer equation in optically thick media, such as the one recently described by Herman *et al.* (1980), one can examine in detail the range of optical depths for which the diffusion domain characteristics are valid. However, the criterion given in (31) is expected to be sufficient. For a cloud with $g = 0.85$, this criterion implies that both τ *and* $\tau_c - \tau$ must be greater than 13 while $\tau_c \geqslant 26$. Since rigorously one would expect the optical depth criterion for the existence of a diffusion domain to be a function of μ_0 and ω_0, in addition to g, it is advantageous to be able to use the measurements themselves to verify that one is in the diffusion domain. This can easily be done by the method outlined below.

Returning to Fig. 10 one sees that the sensitivity of the intensity ratio to s (and hence ω_0) increases as a function of $(1-g)(\tau_c - \tau)$, particularly for small absorption ($s \ll 1$). As absorption increases, the intensity ratio becomes less sensitive to $(1-g) \times (\tau_c - \tau)$ approaching rapidly the limit for a semi-infinite atmosphere, *viz.*, D. For conservative scattering ($s = 0$, $\omega_0 = 1$), the intensity ratio still has not reached the semi-infinite limit of $D = 1$ at the very large value $(1-g)(\tau_c - \tau) = 100$. This implies that at the mid-level of a conservatively scattering cloud of total optical thickness $\tau_c = 200/(1-g)$, the intensity ratio is still 2% less than for a semi-infinite cloud. All of these observations are consistent with those made previously, both in the discussion of Fig. 3 and in the interpretation of (21) and (22). Eqs. (21) and (22), together with (23) and the functions represented by (28), (30) and Table 1, can describe all of the curves presented in Fig. 10 for $(1-g)(\tau_c - \tau) \geqslant 2.5$ to the width of the lines in the figure. This permits an easy interpretation of spectral measurements of the zenith and nadir intensities within a cloud for any arbitrary surface albedo, without resorting to time consuming radiative transfer computations.

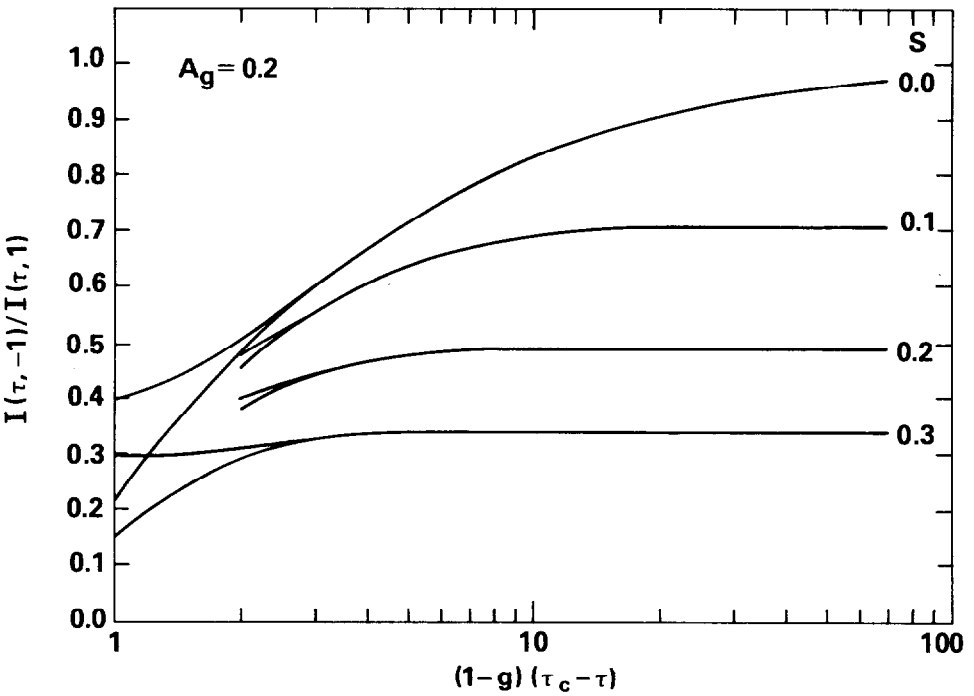

FIG. 10. Ratio of the zenith to nadir propagating intensities at any arbitrary level τ within the diffusion domain of a cloud as a function of $(1 - g)(\tau_c - \tau)$ and s. These curves apply to a ground albedo $A_g = 0.2$ and are insensitive to solar zenith angle for $(1 - g)(\tau_c - \tau) \geq 2.5$.

By assuming that $\omega_0 = 1$ at the visible wavelength for which the ratio of the zenith to nadir propagating intensities is the largest, and by assuming or otherwise determining A_g, one can determine the scaled optical thickness between the flight level and the base of the cloud $[(1 - g)(\tau_c - \tau)]$. If $(1 - g)(\tau_c - \tau)$ is determined to be ≤ 2, then either the cloud is insufficiently thick or the measurements are obtained too *low* within the cloud. Since the intensity must be a linear function of u in the diffusion domain when $\omega_0 = 1$, regardless of the value of the ground albedo [cf. Eqs. (8) and (12)], an angular scan from nadir to zenith can further be used to verify that the observations are indeed within the diffusion domain. If the angular distribution of the intensity is nonlinear, and especially if it is non-monotonic, this provides additional evidence that the cloud is insufficiently thick or the measurements are obtained too *high* within the cloud. If $(1 - g)(\tau_c - \tau) \geq 2$ and the relative intensity is linear in u, then this value of $(1 - g) \times (\tau_c - \tau)$ can be used to interpret measurements at other wavelengths since this function is expected to be nearly wavelength independent, and since the intensity ratio becomes insensitive to this function as absorption increases. With $(1 - g)(\tau_c - \tau)$ thus determined it is clear from Fig. 10 that the similarity parameter s can readily be determined as a function of wavelength. For wavelengths within molecular absorption bands, wavelengths for which $(1 - g)(\tau_c - \tau)$ will be much larger than that previously determined, absorption will be so large that the intensity ratio is insensitive to $(1 - g)(\tau_c - \tau)$. As a direct consequence little error would arise from neglecting the wavelength dependence of $(1 - g)(\tau_c - \tau)$.

If one assumes a value of A_g which is seriously in error, such as 0.0 or 0.4, rather than 0.2, the inferred value of $(1 - g)(\tau_c - \tau)$ under the assumption of conservative scattering would also be in error (see Table 2). However, the resulting curve of $I(\tau, -1)/I(\tau, 1)$ as a function of s would be essentially indistinguishable for all three of these cases. As a consequence no errors would result in the inference of s from spectral measurements of the zenith and nadir propagating intensities within a cloud. The explanation for the near cancellation of the effects of ground reflection and cloud optical thickness can readily be understood. By associating the wavelength for which the intensity ratio is a maximum with conservative scattering, the measurement of $I(\tau, -1)/I(\tau, 1)$ has a fixed value at $s = 0.0$ irrespective of the values of A_g and $(1 - g)(\tau_c - \tau)$[0.7162 in the example presented in Table 2]. At values of $s \geq 0.3$ all curves of $I(\tau, -1)/I(\tau, 1)$ as a function of s must coincide, since the intensity ratio becomes insensitive to A_g and $(1 - g)(\tau_c - \tau)$ [see Figs. 3 and 10]. Since the derivative of the intensity ratio with respect to s near $s = 0.3$ must be nearly the same for all cases, and since the value of the intensity ratio at

TABLE 2. Values of the intensity ratio $I(\tau, -1)/I(\tau, 1)$ as a function of similarity parameter for three different values of the ground albedo when the intensity ratio has a fixed value at $s = 0.0$ of 0.7162.

Similarity parameter	$I(\tau, -1)/I(\tau, 1)$		
	$A_g = 0.0$	$A_g = 0.2$	$A_g = 0.4$
0.0	0.7162	0.7162	0.7162
0.1	0.6400	0.6400	0.6405
0.2	0.4839	0.4841	0.4852
0.3	0.3396	0.3397	0.3402
0.4	0.2279	0.2279	0.2280
0.5	0.1457	0.1457	0.1457
0.6	0.0868	0.0868	0.0868
0.7	0.0460	0.0460	0.0460
0.8	0.0197	0.0197	0.0197
0.9	0.0051	0.0051	0.0051
Inferred value of $(1 - g)(\tau_c - \tau)$	5.33	5.00	4.44

$s = 0.0$ is fixed, little difference in the solution results from ambiguity in A_g. As the value of $(1 - g)(\tau_c - \tau)$ increases from 5.0 to larger values, the intensity ratio $I(\tau, -1)/I(\tau, 1)$ becomes even less sensitive to uncertainties in the ground albedo than in the present example.

In order to relate spectral values of s to the physically important parameter ω_0, it is necessary to determine or otherwise estimate the asymmetry factor g. This can be accomplished by measuring the cloud particle size distribution from the same aircraft platform as the radiation measurements, from which g can easily be computed. A second advantage, though less obvious, results from the simultaneous measurement of the cloud particle size distribution. From this information the single scattering albedo as a function of wavelength can be computed under the assumption that only liquid (or ice) particles, water vapor and known absorbing gases contribute to the absorption of solar radiation by clouds. A comparison of the measurements with theoretical calculations would thus help to estimate the magnitude of any anomalous absorption, if present.

Finally it should be noted that the intensity arising from multiple scattering within a cloud is, for all practical purposes, a function *only* of A_g, $(1 - g)(\tau_c - \tau)$ and s, not only for intensities in the zenith and nadir directions but also for all other directions. This eliminates any possibility of looking at the intensity field at additional angles for the express purpose of determining g. In fact, the choice of similarity parameter defined by (24) was specifically selected with this aim in mind (see van de Hulst, 1980). The degree of polarization, which is necessarily zero in the zenith and nadir directions, has a maximum at different observation angles depending on the value of g when $\omega_0 < 1$ (see, e.g., Kattawar and Plass, 1976), but the utilization of this characteristic would unnecessarily complicate the method described above. For conservative scattering the radiation within the diffusion domain is everywhere unpolarized.

6. Summary and conclusions

A method has been presented for inferring the single scattering albedo of clouds as a function of wavelength from aircraft measurements of the zenith and nadir propagating intensities deep within a cloud layer. This method is based on the radiation properties of the diffusion domain, a region of sufficient distance from both the top and bottom boundaries of a cloud that the diffuse radiation field assumes an asymptotic form characterized by rather simple properties. In this region of an optically thick medium, the relative angular distribution of the intensity is a function of single scattering albedo, cloud asymmetry factor, ground albedo, optical depth level of the measurements, and the optical thickness of the cloud.

As illustrated by the family of curves in Fig. 3, the ratio of the zenith to nadir propagating intensities deep within a cloud layer decreases with increasing absorption $[(1 - \omega_0)^{1/2}]$, increases with surface reflection (A_g), increases with total optical thickness (τ_c), and shows very little sensitivity to the ground albedo or single scattering albedo (ω_0) for large absorption. The dependence of the internal intensity ratio on τ_c, which is illustrated in Fig. 3 for the mid-level $\tau = \tau_c/2$, is such that the important parameter is the *difference* in optical depth between the base of the cloud and any arbitrary level within the diffusion domain of the cloud. Thus Fig. 3 implies that the intensity ratio increases with height, particularly when absorption is small, and is less sensitive to ground reflection high in a cloud than low in a cloud.

In addition to A_g, $(\tau_c - \tau)$ and ω_0, the diffuse radiation field inside a cloud is necessarily a function of the cloud asymmetry factor g. Examination of the sensitivity of the internal intensity ratio to each of these four parameters has led to the conclusion that the single scattering albedo and cloud asymmetry factor affect the radiation field through a coupled dependence on a similarity parameter. Figs. 4–9 demonstrate that each of the constants arising in the asymptotic expression for the internal intensity ratio of very thick layers is a strong function of the similarity parameter s, at least for the range of asymmetry factors expected in terrestrial clouds (*viz.*, $0.80 \leq g \leq 0.90$). As a consequence of these similarity relations coupling ω_0 and g, the internal intensity ratio is shown to be reduced to a function only of A_g, $(1 - g)(\tau_c - \tau)$ and s. A method is described whereby spectral measurements of the zenith and nadir propagating intensities can be

used to determine the similarity parameter as a function of wavelength. Since the total absorption of a cloud layer is a function of the similarity parameter and not of ω_0 and g separately, the similarity parameter is a useful function to be determined. If the cloud particle size distribution is measured at the same time and from the same aircraft platform as the spectral radiometer measurements, the cloud asymmetry factor can easily be computed and used to transform the similarity parameter spectrum to a single scattering albedo spectrum. Although the ground albedo enters the solution explicitly, uncertainties in the value of the ground albedo can be compensated by uncertainties in $(1 - g)(\tau_c - \tau)$, such that the inference of the similarity parameter and single scattering albedo spectra is largely independent of this uncertainty.

The principal assumptions on which the technique is based are 1) that conservative scattering occurs at some wavelength or number of wavelengths in the visible wavelength region, 2) that measurements of the zenith and nadir propagating intensities are made at sufficient distance from the cloud boundaries that the characteristics of the diffusion domain are established, and 3) that the cloud has a sufficient horizontal extent so that the horizontal cloud boundaries do not appreciably affect the internal radiation field. At wavelengths in the visible region where molecular absorption is negligible (see Table 1 of King *et al.*, 1980) and where liquid (or ice) particles have negligible absorption, the only additional absorbers of solar radiation by clouds are aerosol particles within the cloud volume. As a consequence of this absorption clouds will be slightly nonconservative with $1 - \omega_0 \ll 1$. Although the intensity ratio is generally sensitive to absorption for small absorption this ceases to be the case for $1 - \omega_0 \leq 10^{-4}$ (cf. Fig. 3) so that little error would arise by neglecting this small absorption in subsequent analysis. The magnitude of the intensity ratio in the visible wavelength region can be used to assess whether the aircraft flight level is within the diffusion domain, since the intensity ratio for conservative scattering permits a determination of $(1 - g)(\tau_c - \tau)$, a parameter which must be ≥ 2 to guarantee that the measurements are made sufficiently far from the base of the cloud. A measurement of the relative angular distribution of the intensity from nadir to zenith can further be used to assess whether the observations are made far enough from the top boundary of the cloud to be within the diffusion domain. The requirement of a horizontally extensive cloud can be met by judiciously selecting the clouds to be observed. Even for clouds of limited horizontal extent, for which one would expect to have diffusion streams propagating horizontally as well as vertically, the influence of the horizontal diffusion streams can be diminished by making measurements under conditions of small solar zenith angles (high sun). Although the analysis is simplified if A_g is independent of wavelength, this is not a necessary assumption. The effect of small-scale horizontal and vertical inhomogeneities on the internal intensity ratio in real clouds can best be assessed by making field observations.

Acknowledgments. The author is grateful to Dr. R. S. Fraser for reviewing the manuscript and providing helpful comments, to Drs. J. A. Weinman and R. Davies for valuable comments and numerous discussions concerning the research techniques, and to Mr. H. G. Meyer for making the computations.

REFERENCES

Bevington, P. R., 1969: *Data Reduction and Error Analysis for the Physical Sciences*. McGraw-Hill, 336 pp.

Chandrasekhar, S., 1950: *Radiative Transfer*. Oxford University Press, 393 pp.

Davies, R., 1978: The effect of finite geometry on the three-dimensional transfer of solar irradiance in clouds. *J. Atmos. Sci.*, **35**, 1712–1725.

Davis, J. M., S. K. Cox and T. B. McKee, 1979a: Total shortwave radiative characteristics of absorbing finite clouds. *J. Atmos. Sci.*, **36**, 508–518.

——, —— and ——, 1979b: Vertical and horizontal distributions of solar absorption in finite clouds. *J. Atmos. Sci.*, **36**, 1976–1984.

Hansen, J. E., 1971: Multiple scattering of polarized light in planetary atmospheres. Part I. The doubling method. *J. Atmos. Sci.*, **28**, 120–125.

——, and L. D. Travis, 1974: Light scattering in planetary atmospheres. *Space Sci. Rev.*, **16**, 527–610.

Henyey, L. C., and J. L. Greenstein, 1941: Diffuse radiation in the galaxy. *Astrophys. J.*, **93**, 70–83.

Herman, B. M., W. Asous and S. R. Browning, 1980: A semi-analytic technique to integrate the radiative transfer equation over optical depth. *J. Atmos. Sci.*, **37**, 1828–1838.

Irvine, W. M., 1963: The asymmetry of the scattering diagram of a spherical particle. *Bull. Astron. Inst. Netherlands*, **17**, 176–184.

Kattawar, G. W., and G. N. Plass, 1973: Interior radiances in optically deep absorbing media—I. Exact solutions for one-dimensional model. *J. Quant. Spectrosc. Radiat. Transfer*, **13**, 1065–1080.

——, and ——, 1975: Interior radiances in optically deep absorbing media—III. Scattering from Haze L. *J. Quant. Spectrosc. Radiat. Transfer*, **15**, 61–85.

——, and ——, 1976: Asymptotic radiance and polarization in optically thick media: Ocean and clouds. *Appl. Opt.*, **15**, 3166–3178.

King, M. D., 1979: Determination of the ground albedo and the index of absorption of atmospheric particulates by remote sensing. Part II: Application. *J. Atmos. Sci.*, **36**, 1072–1083.

——, D. M. Byrne, J. A. Reagan and B. M. Herman, 1980: Spectral variation of optical depth at Tucson, Arizona between August 1975 and December 1977. *J. Appl. Meteor.*, **19**, 723–732.

McKee, T. B., and S. K. Cox, 1974: Scattering of visible radiation by finite clouds. *J. Atmos. Sci.*, **31**, 1885–1892.

——, and ——, 1976: Simulated radiance patterns for finite clouds. *J. Atmos. Sci.*, **33**, 2014–2020.

Mel'nikova, I. N., 1978: The field of scattered solar radia-

tion in a cloud layer. *Izv. Atmos. Oceanic. Phys.*, **14**, 928–931.

Reynolds, D. W., T. H. Vonder Haar and S. K. Cox, 1975: The effect of solar radiation absorption in the tropical troposphere. *J. Appl. Meteor.*, **14**, 433–444.

Sobolev, V. V., 1975: *Light Scattering in Planetary Atmospheres* (Transl. by W. M. Irvine). Pergamon Press, 256 pp.

Stephens, G. L., 1978a: Radiation profiles in extended water clouds. I: Theory. *J. Atmos. Sci.*, **35**, 2111–2122.

——, 1978b: Radiation profiles in extended water clouds. II: Parameterization schemes. *J. Atmos. Sci.*, **35**, 2123–2132.

——, G. W. Paltridge and C. M. R. Platt, 1978: Radiation profiles in extended water clouds. III: Observations. *J. Atmos. Sci.*, **35**, 2133–2141.

Twomey, S., 1972: The effect of cloud scattering on the absorption of solar radiation by atmospheric dust. *J. Atmos. Sci.*, **29**, 1156–1159.

——, 1974: Pollution and the planetary albedo. *Atmos. Environ.*, **8**, 1251–1256.

——, 1976: Computations of the absorption of solar radiation by clouds. *J. Atmos. Sci.*, **33**, 1087–1091.

——, 1977: The influence of pollution on the shortwave albedo of clouds. *J. Atmos. Sci.*, **34**, 1149–1152.

——, and K. J. Seton, 1980: Inferences of gross microphysical properties of clouds from spectral reflectance measurements. *J. Atmos. Sci.*, **37**, 1065–1069.

van de Hulst, H. C., 1968a: Radiative transfer in thick atmospheres with an arbitrary scattering function. *Bull. Astron. Inst. Netherlands*, **20**, 77–86.

——, 1968b: Asymptotic fitting, a method for solving anisotropic transfer problems in thick layers. *J. Comput. Phys.*, **3**, 291–306.

——, 1974: The spherical albedo of a planet covered with a homogeneous cloud layer. *Astron. Astrophys.*, **35**, 209–214.

——, 1980: *Multiple Light Scattering. Tables, Formulas, and Applications*, Vols. 1 and 2. Academic Press, 739 pp.

Wiscombe, W. J., 1976: On initialization, error and flux conservation in the doubling method. *J. Quant. Spectrosc. Radiat. Transfer*, **16**, 637–658.

——, 1977: Doubling initialization revisited. *J. Quant. Spectrosc. Radiat. Transfer*, **18**, 245–248.